Pergamon

Int. J. Heat Mass Transfer. Vol. 38, No. 15, pp. 2809–2819, 1995
Elsevier Science Ltd
Printed in Great Britain
0017–9310/95 $9.50+0.00

0017–9310(95)00022–4

A new unified *a posteriori* error estimator for adaptive finite element analysis of coupled transport problems

LEANDRO S. OLIVEIRA and KAMYAR HAGHIGHI†

Department of Agricultural Engineering, Purdue University, W. Lafayette, IN 47907-1146, U.S.A.

(*Received* 4 *March* 1994 *and in final form* 27 *December* 1994)

Abstract—In this study, a new error estimator for coupled transport equations has been developed and successfully implemented. The error norm, based on the definition of the energy norm for the system of coupled equations, is evaluated and used in the process of error estimation and calculation of the sizes of the elements in the adapted mesh. A new adaptive strategy for transient problems was also implemented. The performance of the proposed methodology is evaluated by applying it to selected examples. The results showed that the proposed error estimator is suitable for this type of analysis. The adaptive strategy utilized has proved to be efficient, avoiding unnecessary remeshings.

INTRODUCTION

Coupled problems are very common in the studies of simultaneous heat and mass transfer in porous media. Simultaneous heat and mass transfer due to the occurrence of temperature and moisture gradients within a solid body is often encountered in many technological processes. The determination of temperature and moisture distributions in porous solids is essential for equipment and process design, product quality improvement, and the evaluation of storage and handling practices. Some examples of simultaneous heat and mass transfer processes include the drying of cereal grain, foodstuffs, timber, paper, ceramics, clay brick, moisture migration in soils, freeze-drying of biological materials, and chemical vapor transport in crystal growth.

Considerable work has been done in the past decades on the development of sophisticated mathematical models of the simultaneous heat and mass transfer in porous bodies [1–4]. Most of these models are based on systems of coupled nonlinear partial differential equations where temperature and some kind of moisture potential are the primary variables. In most cases, the analytical solution of these equations cannot be determined and an approximate solution technique must be used. The finite element method is a powerful numerical technique capable of solving such complex problems. This numerical technique has been successfully used to simulate coupled transport problems [5–16].

It is well established in the literature that the use of adaptive techniques can increase the accuracy and reliability of finite element solutions [17]. The objective of an adaptive procedure is to enhance the quality of the finite element solutions by continuously redefining the mesh and reducing the discretization error until the solution converges to the desired accuracy. In recent years, there has been a great deal of research effort put into the development of efficient adaptive finite element procedures. Researches in this area are primarily concerned with the development of reliable and computationally inexpensive error estimates for finite element computations. An extensive review on this subject was presented by Noor and Babuska [18]. These estimates play an important role in the development and implementation of an adaptive finite element procedure.

Up to now most of the work done on *a posteriori* error estimates and adaptive procedures is concerned with linear uncoupled problems. An extensive work on linear elasticity problems has been published [19–23]. The adaptive finite element method has also been applied to nonlinear problems [24–28]. The magnitude of the error depends on the exact solution of the problem, since the magnitude is a measure of the 'distance' between the approximate and exact solutions. However, in most real-world applications, the exact solution is not available and must be estimated. Zienkiewicz and Zhu [19] showed that globally smoothed values of stresses representing a higher-order approximation of the original stresses obtained from a finite element analysis could be used instead of the exact solution to calculate the error. This smoothing procedure was successfully used by Huang and Lewis [29] in their adaptive finite element methodology for steady-state heat transfer problems.

Finite element solutions for transient problems have also been improved by adaptive techniques. In an application to wave propagation problems, Lohner [30] used a modified form of the classic interpolation estimates used for steady-state computations in an

†Author to whom correspondence should be addressed.

NOMENCLATURE

C	constant
c_m	mass capacity
c_q	heat capacity
$\|E\|$	exact energy norm
e	error vector
$\|e\|$	error in the energy norm
h	element size
h_m	mass transfer coefficient
h_q	heat transfer coefficient
J_m	mass flux
J_q	heat flux
K	diffusivity
L	differential operator
L_1, L_2	constants
M	number of elements in a mesh
N	shape function
n	surface outward normal
ne	number of nodes per element
P	polynomial degree
T	temperature
t	time
U	moisture potential
v	vector of dependent variables
x, y	Cartesian coordinates.

Greek symbols

α_q	convective heat transfer coefficient
α_u	convective mass transfer coefficient
Γ	boundary surface
δ	thermo-gradient coefficient
ε	phase conversion factor
η	relative error
$\bar{\eta}$	target relative error
λ	latent heat
ξ	refinement variable
ρ	density
ϕ_1, ϕ_2	generic transport variables
Ω	domain.

Subscripts and superscripts

0	initial
A	area
e	element
f	final
m	mass
o	previous value
P, S	smoothed
q	heat
s	surface
w	wall
∞	undisturbed fluid.

adaptive finite element scheme for transient problems. Later, he incorporated directional refinement and body motion in the context of adaptive refinement [31]. This directional refinement was a combination of h-refinement and stretching of the elements in the regions where the gradients were very steep. Error estimates based on an interpolation theory were used by Probert *et al.* [32] in the adaptive procedure to solve a two-dimensional (2D) transient heat conduction problem. Lewis *et al.* [33], in an extension of a previous work [29], also applied the adaptive technique to transient flow problems together with an adaptive time stepping scheme.

There are some studies dealing with error estimation and adaptive analysis for coupled problems available in the literature, but almost all of these efforts deal with equations that are solved sequentially and not simultaneously. An application of error estimation and adaptive techniques to systems of simultaneous coupled differential equations was presented by Trompert [34]. The numerical technique used was the finite difference method and error estimators were developed separately for each equation of the coupled system. Each error estimator presented different behavior, leading to difficulties in establishing a simple and efficient refinement strategy. The development of a single unified error estimator that includes the coupling effects is crucial for the establishment of a more accurate and efficient adaptive procedure.

In this paper, a new, simple, efficient and unified error estimator for coupled transport problems is presented. The error norm, based on the definition of the energy norm for the system of coupled partial differential equations, was evaluated and used in the process of error estimation and calculation of the size of the elements in the adapted mesh. Unlike other error estimators for systems of coupled equations [34], this new estimator is based on the system of equations and not on each transport equation separately. With that, the problem of having different error behavior for different equations in the system is overcome. An adaptive h-refinement procedure was also used in this study. Two example problems were studied to demonstrate the technique.

THEORETICAL CONSIDERATIONS

This section presents the formulation for error estimation and the general procedure for implementing the adaptive analysis for coupled transport problems. Although the concept of energy norm, formulated by Zienkiewicz and Zhu [19], is used here, the development of the error in the energy norm for coupled transport problems and its implementation is totally new and unique to this work.

Coupled transport equations

In a generalized form, the system of coupled transport equations can be written as

$$c_q \frac{\partial T}{\partial t} = \nabla(k_{11}\nabla T + k_{12}\nabla U) \tag{1}$$

$$c_m \frac{\partial U}{\partial t} = \nabla(k_{21}\nabla T + k_{22}\nabla U) \tag{2}$$

where $T = T^* - T_\infty$ is the normalized temperature, $U = U^* - U_\infty$ is the normalized moisture potential, T^* is the temperature, U^* is the moisture potential, T_∞ is the air temperature, U_∞ is the air moisture potential, k_{11}, k_{12}, k_{21}, k_{22} are the diffusivities, and c_q and c_m are the heat and mass capacities, respectively.

The generalized boundary conditions are given by

$$c_{11}k_{11}\frac{\partial T}{\partial n} + c_{12}k_{12}\frac{\partial U}{\partial n} + c_{1q}h_q T + c_{1m}h_m U + j_q = 0 \quad \text{on } \Gamma_i \quad i = 1, 2\ldots \tag{3}$$

$$c_{21}k_{21}\frac{\partial T}{\partial n} + c_{22}k_{22}\frac{\partial U}{\partial n} + c_{2q}h_q T + c_{2m}h_m U + j_m = 0 \quad \text{on } \Gamma_i \quad i = 1, 2\ldots \tag{4}$$

where h_q is the heat transfer coefficient, h_m is the mass transfer coefficient, n is the surface outward normal, j_q is a known heat flux, j_m is a known mass flux, and c_{ij}, $i, j = 1, 2$, are constants that can be either 0 or 1, and c_{iq} and c_{im}, $i = 1, 2$, are known constants that will depend on the model used; Γ_i, $i = 1, 2\ldots$, represent boundary surfaces.

Error estimation

In Galerkin's weighted residual method, the dependent variables T and U are approximated by interpolating functions in terms of the known nodal values T_j and U_j:

$$T \approx \bar{T} = \sum_{j=1}^{n} N_j(x, y)T_j(t) \tag{5}$$

$$U \approx \bar{U} = \sum_{j=1}^{n} N_j(x, y)U_j(t) \tag{6}$$

where $\bar{T}$ and $\bar{U}$ are the approximated values of the temperature and moisture potential, and the N_j's are the basis functions.

The error in the finite element solution can be expressed as

$$\mathbf{e} = \begin{bmatrix} T - \bar{T} \\ U - \bar{U} \end{bmatrix}. \tag{7}$$

The pointwise definition of error as given in equation (7) is difficult to implement and, in general, norms and semi-norms are used instead [19]. One of the most common norms is the *energy norm*. The energy norm has proved to be very effective in diffusion problems [29] and can be written in general form as

$$\|e\| = \left(\int_\Omega \mathbf{e}^T L \mathbf{e}\, d\Omega\right)^{1/2} \tag{8}$$

where L is the differential operator. For the coupled system of equations (1) and (2), the differential operator is defined as

$$L = -\begin{bmatrix} \nabla k_{11}\nabla & \nabla k_{12}\nabla \\ \nabla k_{21}\nabla & \nabla k_{22}\nabla \end{bmatrix}. \tag{9}$$

If equations (7) and (9) are substituted in equation (8):

$$\begin{aligned} \|e\|^2 &= -\int_\Omega [T - \bar{T} \quad U - \bar{U}] \\ &\quad \times \begin{bmatrix} \nabla k_{11}\nabla & \nabla k_{12}\nabla \\ \nabla k_{21}\nabla & \nabla k_{22}\nabla \end{bmatrix} \begin{bmatrix} T - \bar{T} \\ U - \bar{U} \end{bmatrix} d\Omega \\ &= -\int_\Omega [T - \bar{T} \quad U - \bar{U}] \\ &\quad \times \begin{bmatrix} \nabla k_{11}\nabla(T - \bar{T}) + \nabla k_{12}\nabla(U - \bar{U}) \\ \nabla k_{21}\nabla(T - \bar{T}) + \nabla k_{22}\nabla(U - \bar{U}) \end{bmatrix} d\Omega \\ &= -\int_\Omega [(T - \bar{T})\nabla k_{11}\nabla(T - \bar{T}) \\ &\quad + (T - \bar{T})\nabla k_{12}\nabla(U - \bar{U}) \\ &\quad + (U - \bar{U})\nabla k_{21}\nabla(T - \bar{T}) \\ &\quad + (U - \bar{U})\nabla k_{22}\nabla(U - \bar{U})]\, d\Omega. \end{aligned} \tag{10}$$

If we apply Green's theorem to equation (10), the error in the energy norm for the coupled transport problem described by equations (1) and (2) can be written as

$$\begin{aligned} \|e\|^2 &= \int_\Omega k_{11}(\nabla T - \nabla \bar{T})^2\, d\Omega + \int_\Omega k_{22}(\nabla U - \nabla \bar{U})^2\, d\Omega \\ &\quad + \int_\Omega (k_{12} + k_{21})(\nabla T - \nabla \bar{T})(\nabla U - \nabla \bar{U})\, d\Omega \\ &\quad - \int_\Gamma (T - \bar{T})\left[k_{11}\left(\frac{\partial T}{\partial n} - \frac{\partial \bar{T}}{\partial n}\right) + k_{12}\left(\frac{\partial U}{\partial n} - \frac{\partial \bar{U}}{\partial n}\right)\right] d\Gamma \\ &\quad - \int_\Gamma (U - \bar{U})\left[k_{21}\left(\frac{\partial T}{\partial n} - \frac{\partial \bar{T}}{\partial n}\right) + k_{22}\left(\frac{\partial U}{\partial n} - \frac{\partial \bar{U}}{\partial n}\right)\right] d\Gamma. \end{aligned} \tag{11}$$

The error in each element is then calculated as follows:

$$\|e\|_e^2 = \int_{A_e} [k_{11}(\nabla T - \nabla \bar{T})^2 + k_{22}(\nabla U - \nabla \bar{U})^2 + (k_{12}+k_{21})(\nabla T - \nabla \bar{T})(\nabla U - \nabla \bar{U})]\,dA - \int_{S_e} (T-\bar{T})\left[k_{11}\left(\frac{\partial T}{\partial n} - \frac{\partial \bar{T}}{\partial n}\right) + k_{12}\left(\frac{\partial U}{\partial n} - \frac{\partial \bar{U}}{\partial n}\right)\right] dS - \int_{S_e} (U-\bar{U})\left[k_{21}\left(\frac{\partial T}{\partial n} - \frac{\partial \bar{T}}{\partial n}\right) + k_{22}\left(\frac{\partial U}{\partial n} - \frac{\partial \bar{U}}{\partial n}\right)\right] dS \tag{12}$$

where A_e is the area of the element, and S_e is the length of the side of the element on the boundary.

In a similar fashion the *exact energy norm* can be defined as

$$\|E\| = \left(\int_\Omega \mathbf{v}^T L \mathbf{v}\, d\Omega\right)^{1/2} \tag{13}$$

where

$$\mathbf{v} = \begin{bmatrix} T \\ U \end{bmatrix} \tag{14}$$

represents the exact solutions of temperature and moisture potential, and L is the differential operator as defined in equation (9). Following the same procedure that led to equation (11), one can obtain for $\|E\|$:

$$\|E\|^2 = \int_\Omega (k_{11}(\nabla T)^2 + k_{22}(\nabla U)^2 + (k_{12}+k_{21})(\nabla T)(\nabla U))\,d\Omega - \int_\Gamma T\left(k_{11}\frac{\partial T}{\partial n} + k_{12}\frac{\partial U}{\partial n}\right) d\Gamma - \int_\Gamma U\left(k_{21}\frac{\partial T}{\partial n} + k_{22}\frac{\partial U}{\partial n}\right) d\Gamma. \tag{15}$$

A practical representation of the error in terms of a relative error is

$$\eta = \frac{\|e\|}{\|E\|}. \tag{16}$$

The exact solutions of the dependent variables (temperature and moisture potential) and their gradients are usually not available for this type of problem. For the temperature and moisture gradients, a global 'smoothed' value taken as a higher-order approximation of the value given by the finite element solution can be used instead [29]. The smoothed continuous values of the temperature and moisture gradients in each element, $\partial T^s/\partial x_i$ and $\partial U^s/\partial x_i$, are evaluated in the following way:

$$\frac{\partial T^s}{\partial x_i} = \sum_{j=1}^{ne} N_j \frac{\partial T^p}{\partial x_i} \tag{17}$$

$$\frac{\partial U^s}{\partial x_i} = \sum_{j=1}^{ne} N_j \frac{\partial U^p}{\partial x_i} \tag{18}$$

where ne is the number of nodes per element, N_j are the shape functions used in the finite element analysis, $\partial T^p/\partial x_i$ and $\partial U^p/\partial x_i$ are the unknown smoothed nodal values obtained by imposing the following constraints:

$$\int_\Omega N^T\left(\frac{\partial T^s}{\partial x_i} - \frac{\partial \bar{T}}{\partial x_i}\right) d\Omega = 0 \tag{19}$$

$$\int_\Omega N^T\left(\frac{\partial U^s}{\partial x_i} - \frac{\partial \bar{U}}{\partial x_i}\right) d\Omega = 0 \tag{20}$$

in which $\partial \bar{T}/\partial x_i$ and $\partial \bar{U}/\partial x_i$ are the gradient values obtained from the original finite element analysis. Application of equations (19) and (20) to all the elements in the domain leads to the following systems of equations:

$$\int_A N^T N\,dx\,dy \left\{\frac{\partial T^p}{\partial x_i}\right\} = \int N^T \frac{\partial \bar{T}}{\partial x_i} dx\,dy \tag{21}$$

$$\int_A N^T N\,dx\,dy \left\{\frac{\partial U^p}{\partial x_i}\right\} = \int N^T \frac{\partial \bar{U}}{\partial x_i} dx\,dy \tag{22}$$

where $\partial T^p/\partial x_i$ and $\partial U^p/\partial x_i$ are the smoothed gradients. Systems (21) and (22) are solved to find the globally smoothed values of the temperature and moisture gradients.

An approximation for the exact value of the dependent variable in the boundary integrals was developed by Franca and Haghighi [35]. This approximation is taken as a higher-order approximation than the finite element solution. A similar approach was adopted in this study. The values of T and U on the boundary are taken as the solution of the system of equations given by boundary conditions (3) and (4):

$$c_{1q}h_q T + c_{1m}h_m U = -\left(c_{11}k_{11}\frac{\partial T}{\partial n} + c_{12}k_{12}\frac{\partial U}{\partial n} + j_q\right) \tag{23}$$

$$c_{2q}h_q T + c_{2m}h_m U = -\left(c_{21}k_{21}\frac{\partial T}{\partial n} + c_{22}k_{22}\frac{\partial U}{\partial n} + j_m\right) \tag{24}$$

where $\partial T/\partial n$ and $\partial U/\partial n$ are the smoothed temperature and moisture gradients given by the solution of the system of equations (21) and (22).

In the case of the integrals containing the finite element solution gradients, the boundary conditions (3) and (4) are used to give

$$c_{11}k_{11}\frac{\partial \bar{T}}{\partial n}+c_{12}k_{12}\frac{\partial \bar{U}}{\partial n}=-(c_{1q}h_q\bar{T}+c_{1m}h_m\bar{U}+j_q) \tag{25}$$

and

$$c_{21}k_{21}\frac{\partial \bar{T}}{\partial n}+c_{22}k_{22}\frac{\partial \bar{U}}{\partial n}=-(c_{2q}h_q\bar{T}+c_{2m}h_m\bar{U}+j_m). \tag{26}$$

The solution of system of equations (23) and (24), and equations (25) and (26) are substituted in equation (12) in the calculation of the error in each element. Similarly, the solution of system of equations (23) and (24) are substituted in equation (15) for the evaluation of the exact energy norm.

Adaptive procedure

The approximate errors in each element can be evaluated by using the smoothed temperature and moisture gradients in equations (12). The total error is then related to the individual element contributions by

$$\|e\|^2=\sum_{e=1}^{M}\|e\|_e^2. \tag{27}$$

The requirement for an optimum mesh is that all the elements of the mesh must have approximately equal error distribution [19, 29]. If we distribute $\|E\|^2$ equally over all the elements, the average error per element can be estimated as

$$\|\bar{e}\|_e^2=\frac{\eta\|E\|^2}{M}. \tag{28}$$

If $\bar{\eta}$ is a pre-specified limit for the percentage error, then the error in each element is bounded by

$$\|\bar{e}\|_e^2\leqslant\frac{\bar{\eta}\|E\|^2}{M} \tag{29}$$

where M is the total number of elements in the mesh. If we define a new variable ξ as

$$\xi=\frac{\|e\|_e}{\|\bar{e}\|_e} \tag{30}$$

we can then establish a criterion for mesh refinement and derefinement. Whenever $\xi>1$ the mesh will be refined; otherwise, the mesh will be coarsened. The predicted size of the new element can be calculated from the current element size:

$$h_e=h_e^o/\xi^{1/p} \tag{31}$$

where h_e is the predicted new element size, h_e^o is the current element size and p is the polynomial order of the shape functions.

IMPLEMENTATION

A finite element code was developed for the solution of coupled transport problems and implemented on a Sun 2 SPARCstation. A subroutine for error estimation and evaluation of the size of the new mesh is included in the code. The program, including the adaptive remeshing, is fully automatic and the user is only required to build the initial coarse mesh. The software INTELMESH© developed by Kang and Haghighi [36] was used for the mesh generation. It generates the nodes in the problem domain using the concept of wave propagation. The mesh generator allows the user to specify the size of the elements around the critical points.

The present implementation of the adaptive strategy for transient coupled problems works in the following way: for each N advances in time (N is an user defined constant), after the finite element analysis is performed, the overall solution error is evaluated from equation (16). If η is greater than a pre-specified limit, then the sizes of the elements in the new adapted mesh are computed from equation (31). The refinement process is carried out by using the centroid of each element of the original mesh as a critical point in the adapted mesh generation process. The evaluated size of each element will be the size of the new mesh around each critical point, and the grading of the mesh is controlled by the wave propagation rate in the mesh generation process. The interpolation of the nodal information from one mesh to another is carried out using the same shape functions used in the finite element approximation of the variables. The adaptive strategy used in this study is described in detail in Oliveira *et al.* [37]. The adaptive time stepping methodology developed by Gresho *et al.* [38], and modified by Bixler [39] was implemented. The formulation for time step size prediction takes into account both temperature and moisture potential rates of change as well as the mesh size.

To illustrate the numerical performance of the proposed formulation, two example problems were selected and successfully implemented. The error in the finite element solution for transient coupled transport problems was estimated, and its variation in time is presented. There are no analytical solutions available for both examples. The numerical results obtained in this study were compared to other numerical solutions available in the literature. All finite element models for the analyses consisted of linear triangular elements.

Example 1. For this example, a generic system of two coupled differential equations was adopted and solved. The equations used have the following format:

$$c_1\frac{\partial\phi_1}{\partial t}=K_{11}\nabla^2\phi_1+K_{12}\nabla^2\phi_2+L_1\frac{\partial C}{\partial y} \tag{32}$$

$$c_2\frac{\partial\phi_2}{\partial t}=K_{21}\nabla^2\phi_1+K_{22}\nabla^2\phi_2+L_2\frac{\partial C}{\partial y} \tag{33}$$

where ϕ_1 and ϕ_2 are the dependent variables, c_1 and c_2 are the capacities, K_{11}, K_{12}, K_{21} and K_{22} are the conductivities, L_1 and L_2 are constants, and C is a property of the medium. The equations format resembles the transport equations used to describe

Table 1. Coefficients of the equations in Example 1

Property	Value	Property	Value
K_{11}	1×10^{-1}	L_1	0.0
K_{12}	2×10^{-5}	L_2	1.0
K_{21}	2×10^{-5}	c_1	1.0
K_{22}	5×10^{-2}	c_2	1.0
C	1×10^{-2}		

heat and mass transfer in saturated soils, where gravitational effects are taken into account [9]. The values for the coefficients involved are presented in Table 1. The schematic diagram of the problem with imposed initial and boundary conditions is shown in Fig. 1(a).

The initial coarse mesh was arbitrarily generated and is shown in Fig. 1(b). NON and NOE stand for the number of nodes and the number of elements, respectively. The first adapted mesh is generated after the first advance in time and is presented in Fig. 1(c). The mesh is more refined close to the inclined surface, where the geometrical and boundary conditions

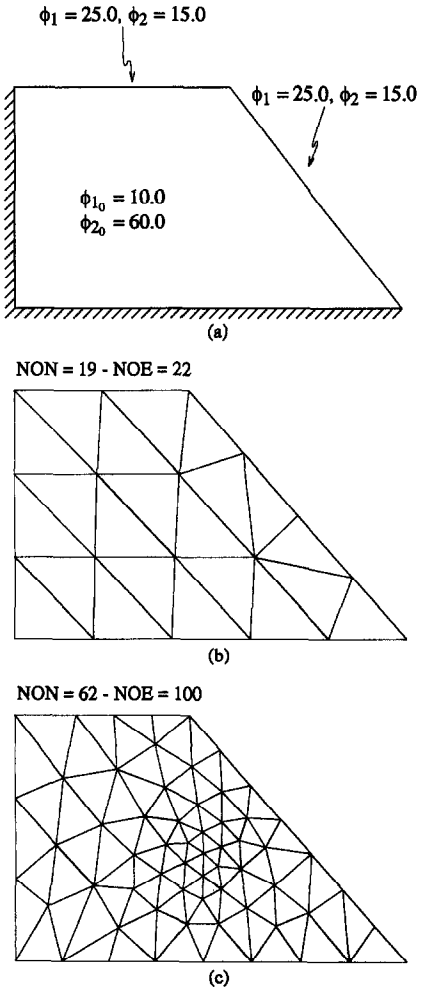

Fig. 1. (a) Schematic diagram of Example 1, (b) initial mesh and (c) adapted mesh for $t_f = 1.0$.

effects are more accentuated. The specified target error was $\bar{\eta} = 0.15$.

The contour plots for the dependent variables ϕ_1 and ϕ_2 are presented in Figs. 2(a) and (b), respectively. Both distributions agree with the expected behavior. The influence of the boundary conditions along the inclined surface is clearly seen as it forces the contour lines to shift downwards in the lower part of the domain. Figure 3(a) shows the time step size variation with time. The time step size increases at the beginning, reaches a maximum, then decreases monotonously, staying almost constant until the final time is reached. The time step size decreases in response to a decrease in the element size after the first adaptive remeshing. The analysis was completed after 257 time steps. The error variation with time is presented in Fig. 3(b). The estimated error decreases very fast at the beginning, approaching a constant value for the remaining time at a much slower rate. No more than one remeshing was necessary, since the error reached the specified tolerance at the beginning of the process.

Example 2. The second example studied was that of a rectangular timber slab under convective drying [Fig. 4(a)]. Due to the symmetry of the problem, a quarter of the timber slab was used for the finite element analysis. Symmetry conditions (i.e. zero heat and mass fluxes) were assumed along sides AB and BC, and convective boundary conditions were assumed along sides CD and DA. Luikov's equations for coupled heat and mass transfer in porous body were adopted and solved. If the total pressure is assumed constant throughout the porous body, Luikov's basic conservation equations are

$$\rho c_q \frac{\partial T^*}{\partial t} = \nabla[(k_q + \varepsilon\lambda k_m \delta')\nabla T^* + \varepsilon\lambda k_m \nabla U^*] \quad (34)$$

$$\rho c_m \frac{\partial U^*}{\partial t} = \nabla[k_m \delta' \nabla T^* + k_m \nabla U^*] \quad (35)$$

where $\delta' = \delta/c_m$.

The initial and boundary conditions for equations (34) and (35) are

$$T_i^* = T_0 \quad U_i^* = U_0 \quad (36)$$

$$\frac{\partial T^*}{\partial n} = \frac{\partial U^*}{\partial n} = 0 \quad \text{on} \quad \Gamma_{AB} \text{ and } \Gamma_{BC} \quad (37)$$

$$k_q \frac{\partial T^*}{\partial n} + j_q + \alpha_q (T - T_\infty) + (1-\varepsilon)\lambda\alpha_u (U - U_\infty) = 0$$

$$\text{on} \quad \Gamma_{CD} \text{ and } \Gamma_{DA} \quad (38)$$

$$k_m \frac{\partial U^*}{\partial n} + j_m + k_m \delta' \frac{\partial T^*}{\partial n} + \alpha_u (U - U_\infty) = 0$$

$$\text{on} \quad \Gamma_{CD} \text{ and } \Gamma_{DA}. \quad (39)$$

Equations (34) and (35), and boundary conditions (38) and (39) were nondimensionalized following the

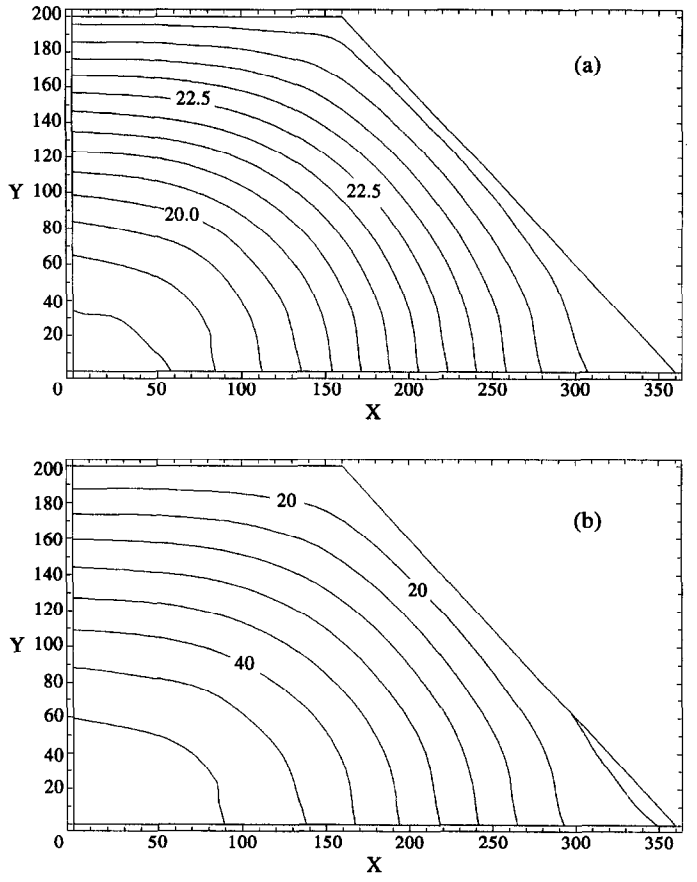

Fig. 2. (a) ϕ_1 and (b) ϕ_2 distribution for $t = 1.0$.

lines of Thomas *et al.* [8]. The discretization of the nondimensionalized form of equations (34) and (35) was based on the application of the Galerkin weighted residual method [40]. The boundary condition and thermophysical properties data are listed in Table 2. The analysis was performed for two different drying times, $t_f = 20$ min and $t_f = 100$ h. The initial conditions were $T_0 = 10°C$ and $U_0 = 100°M$ for both analyses.

For $t_f = 20$ min, the initial coarse mesh, arbitrarily defined by the user, is shown in Fig. 4(b). The first adaptive remeshing was imposed to occur after the first advance in time and the adapted mesh is presented in Fig. 4(c). The adapted mesh is more refined near the upper and right surfaces where the convection takes place, i.e where both temperature and moisture potential gradients are steeper. The prescribed target error was $\bar{\eta} = 0.15$.

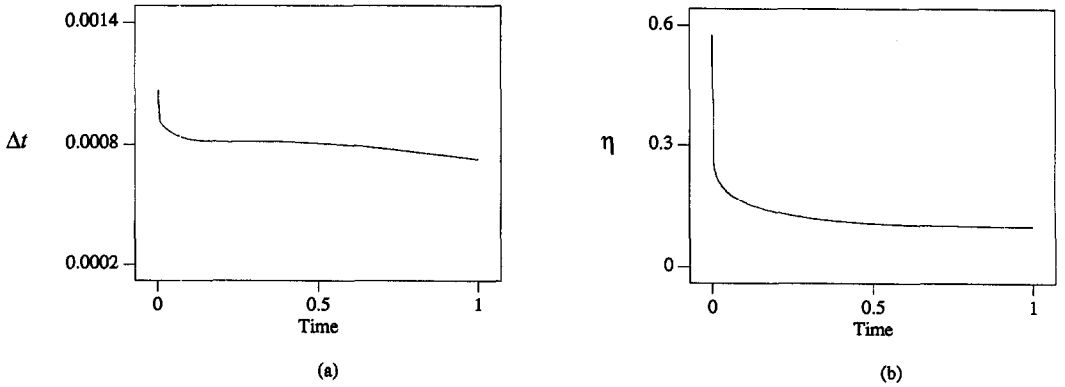

Fig. 3. (a) Time step size variation and (b) error variation in time for $t_f = 1.0$.

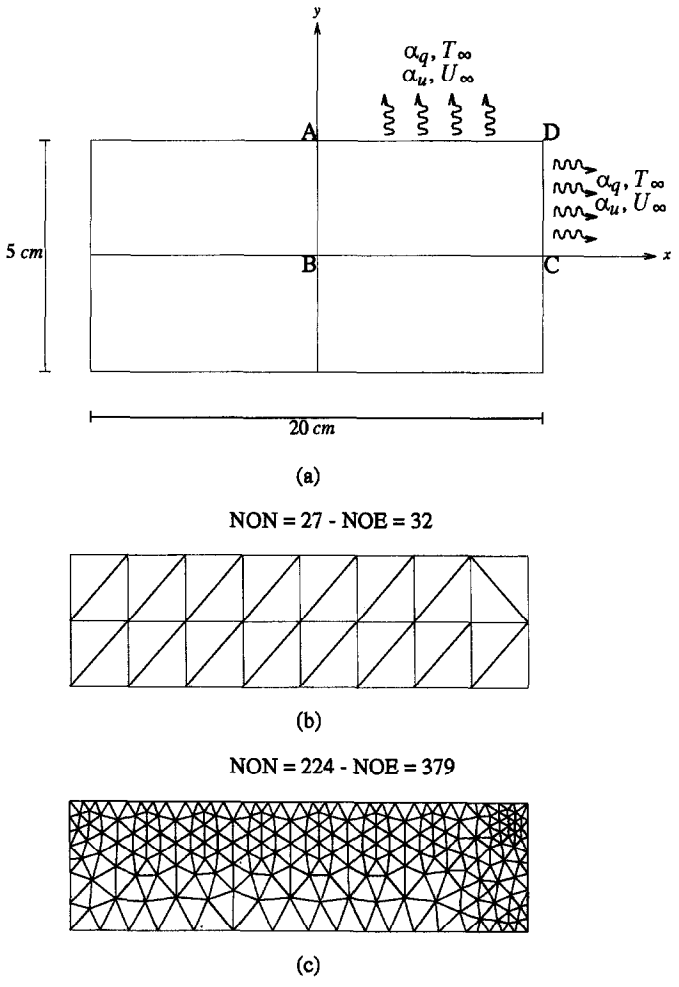

Fig. 4. (a) Schematic diagram of Example 2, (b) initial mesh and (c) adapted mesh for $t_f = 20$ min.

The time step size variation with time is presented in Fig. 5(a). The time step size increases at the beginning, reaches a peak and then suddenly drops. This sudden drop is attributed to a delayed response to the adaptive refinement that occurred after the first advance in time. After the drop, the time step size goes on increasing and stabilizes until the final time is reached. The savings in the time step size were of about 25% of its initial value ($\Delta t_i = 2$ s). The analysis was completed in 489 time steps.

The results of the analysis for temperature variation in the lower left corner of the slab ($x = 0$, $y = 0$) are shown in Fig. 5(b) where they also compared to the results of Thomas *et al.* [8] and Irudayaraj *et al.* [40]. The predicted temperature lies between the predictions of the other two models. The moisture potential variation in the same coordinates ($x = 0$, $y = 0$) was not significant for $t_f = 20$ min.

Figure 5(c) shows the estimated error variation. The error decreases monotonously after the first adaptive refinement reaching a final value of $\eta = 0.084$ at $t_f = 20$ min. Since the error kept decreasing and

Table 2. Boundary condition data and thermophysical properties for Example 2

Property	Value	Unit	Property	Value	Unit
k_q	0.35	$W\,m^{-1}\,K^{-1}$	ρ	500.0	$kg\,m^{-3}$
c_q	1284.0	$J\,kg^{-1}\,K^{-1}$	ε	0.3	
c_m	0.003	$kg\,kg^{-1}\,°M^{-1}$	λ	0.25×10^7	$J\,kg^{-1}$
k_m	1.5×10^{-9}	$kg\,m\,s\,°M^{-1}$	δ	0.02	$°C^{-1}$
α_q	22.5	$W\,m^{-2}\,K^{-1}$	T_∞	60.0	°C
α_u	1.67×10^{-6}	$kg\,m^{-2}\,s\,°M^{-1}$	U_∞	100.0	°M

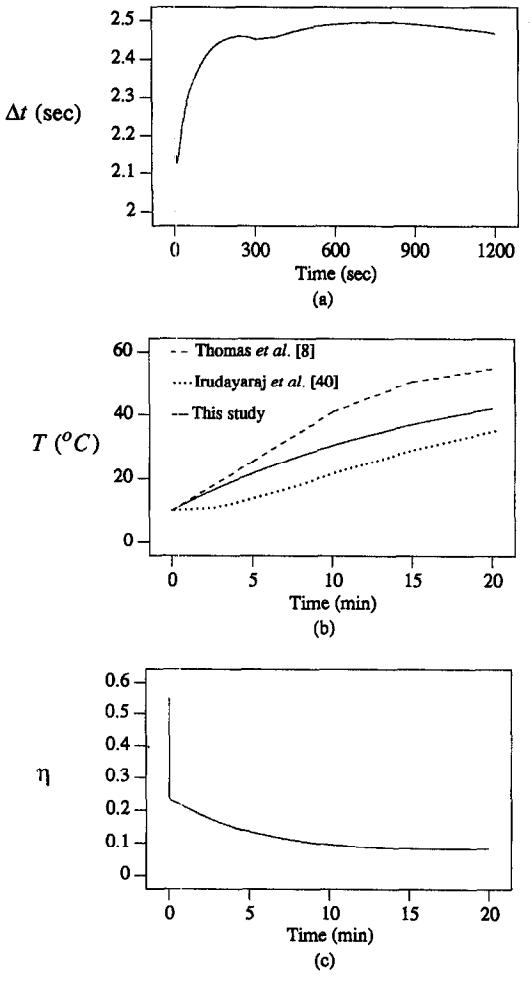

Fig. 5. (a) Time step size variation, (b) temperature variation at $x = 0$ and $y = 0$ and (c) error variation for Example 2, $t_f = 20$ min.

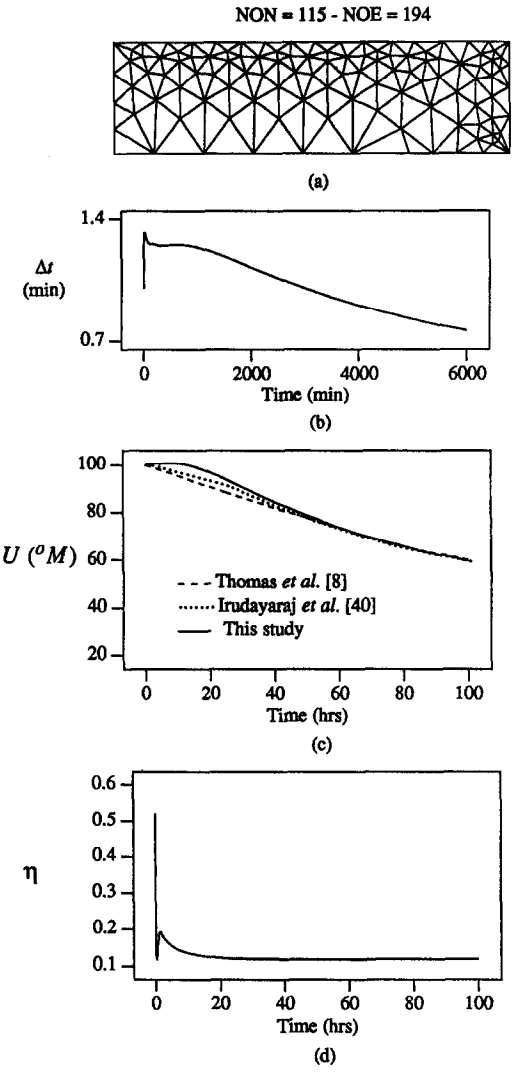

Fig. 6. (a) Adapted mesh, (b) time step size variation, (c) moisture potential variation at $x = 0$ and $y = 0$ and (d) error variation for Example 2, $t_f = 100$ h.

reached the target error ($\bar{\eta} = 0.15$) early, no more adaptive refinements were needed.

In order to demonstrate the influence of the moisture potential variation on the solution error, an analysis for $t_f = 100$ h was performed. The initial coarse mesh used is the same used in the previous analysis ($t_f = 20$ min) and is presented in Fig. 4(b). Figure 6(a) shows the first adapted mesh, after the first time step. Again, the mesh is more refined close to the surfaces where convection takes place. This mesh is less refined than the one obtained in the previous analysis because the target error in this case was higher ($\bar{\eta} = 0.20$).

Figure 6(b) shows the time step size variation. The time step size increases at the beginning, reaches a peak and then have a sudden drop in response to the adaptive refinement. After the drop, the time step size goes on decreasing until the final time is reached.

The predicted moisture potential variation in the lower left corner of the slab is presented in Fig. 6(c). The results are compared to the results of Thomas *et al.* [8] and Irudayaraj *et al.* [40]. The predicted moisture potential rate of change is slower than in the other two models at the beginning and then at about half way to the final time there is no significant difference among the three. The temperature in the slab achieves a steady-state in the early minutes of the drying process and there is no significant variation from then on.

The estimated error variation presents an interesting behavior in this case [Fig. 6(d)]. The error decreases very fast after the adaptive remeshing, reaches a minimum and then goes up, reaches a local maximum and then decreases monotonously approaching a constant value. The peak in the error curve is caused by an increase in the denominator of equation (16) when the contribution of the boundary integrals to the energy norm are most significant. Both temperature and moisture gradients are very high at and close to the boundaries at the beginning. Since the error reached the prescribed error early, no more adaptive remeshings were needed.

CONCLUSIONS

A new, simple and efficient unified error estimator for coupled transport problems was proposed and successfully implemented. This error estimator is very generic and can be applied to any system of coupled transport differential equations. For example, if the total pressure is not constant throughout the porous body, an equation for pressure would have to be added to Luikov's model. The formulation for error evaluation would remain the same. The only difference is that the error vector would contain the pressure error in it. Both the proposed error estimator and adaptive strategy utilized have proved to be very efficient. The desired accuracy was always attained and the adapted meshes agreed with the expected physical behavior, i.e. the meshes were more refined in regions where steeper gradients were expected.

Acknowledgement—Leandro Oliveira wishes to thank the Brazilian government agency CAPES for his scholarship.

REFERENCES

1. J. R. Philip and D. A. de Vries, Simultaneous transfer of heat and moisture in porous media, *Trans. Am. Geophys. Un.* **39,** 909–916 (1957).
2. A. V. Luikov, *Heat and Mass Transfer in Capillary Porous Bodies*. Pergamon Press, Oxford (1966).
3. S. Whitaker, Simultaneous heat, mass and momentum transfer in porous media. A theory of drying in porous media, *Adv. Heat Transfer* **13,** 119–200 (1977).
4. M. Fortes and M. R. Okos, A non-equilibrium thermodynamics approach to transport phenomena in capillary porous media, *Trans. ASAE* **24**(3), 756–760 (1981).
5. R. W. Lewis and R. W. Garner, A finite element solution of coupled electrokinetic and hydrodynamic flow in porous media, *Int. J. Numer. Meth. Engng* **5,** 41–55 (1972).
6. R. W. Lewis, G. Comini and C. Humpheson, Finite element application to heat and mass transfer problems in porous bodies (in Russian), *Inzh. Fiz. Zh.* **29,** 483–489 (1975).
7. G. Comini and R. W. Lewis, A numerical solution of two-dimensional problems involving heat and mass transfer, *Int. J. Heat Mass Transfer* **19,** 1387–1392 (1976).
8. H. R. Thomas, K. Morgan and R. W. Lewis, A fully nonlinear analysis of heat and mass transfer problems in porous bodies, *Int. J. Numer. Meth. Engng* **15,** 1381–1393 (1980).
9. H. R. Thomas, Modelling two-dimensional heat and moisture transfer in unsaturated soils, including gravity effects, *Int. J. Numer. Anal. Meth. Geomech.* **9,** 573–588 (1985).
10. E. Sidiropoulos and C. Tzimopoulos, Sensitivity analysis of a coupled heat and mass transfer model in unsaturated porous media, *J. Hydrol.* **64,** 281–298 (1983).
11. K. Haghighi and L. J. Segerlind, Modeling simultaneous heat and mass transfer in an isotropic sphere—a finite element approach, *Trans. ASAE* **31**(2), 629–637 (1988).
12. K. Haghighi and L. J. Segerlind, Failures of biomaterials subjected to temperature and moisture gradients using the finite element method—I, *Trans. ASAE* **31**(3), 930–937 (1988).
13. K. Haghighi and L. J. Segerlind, Failures of biomaterials subjected to temperature and moisture gradients using the finite element method—II, *Trans. ASAE* **31**(3), 938–946 (1988).
14. R. W. Lewis, P. J. Roberts and B. A. Schrefler, Finite element modelling of two-phase heat and fluid flow in deforming porous media, *Transp. Porous Media* **4,** 319–334 (1989).
15. K. Haghighi, J. Irudayaraj, R. L. Stroshine and S. Sokhansanj, Grain kernel drying simulation using the finite element method, *Trans. ASAE* **33**(6), 1957–1965 (1990).
16. W. J. Ferguson and R. W. Lewis, A fully nonlinear analysis of temperature, moisture content, and pressure in a capillary porous body, *Numer. Heat Transfer B* **23,** 91–110 (1993).
17. O. C. Zienkiewicz and R. L. Taylor, *The Finite Element Method* (4th Edn), Vol. 1. McGraw-Hill, New York (1989).
18. A. K. Noor and I. Babuska, Quality assessment and control of finite element solutions, *Finite Element in Analysis and Design* **3,** 1–26 (1987).
19. O. C. Zienkiewicz and J. Z. Zhu, A simple error estimator and adaptive procedure for practical engineering analysis, *Int. J. Numer. Meth. Engng* **24,** 337–357 (1987).
20. J. Z. Zhu and O. C. Zienkiewicz, Adaptive techniques in the finite element method, *Commun. Appl. Numer. Meth.* **4,** 197–204 (1988).
21. R. Mahnken and E. Stein, Adaptive time-step control in creep analysis, *Int. J. Numer. Meth. Engng* **28,** 1619–1633 (1989).
22. S. Holzer, E. Rank and H. Werner, An implementation of the hp-version of the finite element method for Reissner–Mindlin plate problems, *Int. J. Numer. Meth. Engng* **30,** 459–471 (1990).
23. O. C. Zienkiewicz and J. Z. Zhu, Adaptivity and mesh generation, *Int. J. Numer. Meth. Engng* **32,** 783–810 (1991).
24. F. R. Sledge and W. C. Rheinboldt, A program design for an adaptive, nonlinear finite element solver, *Computers Structures* **20**(1–3), 85–90 (1985).
25. W. C. Rheinboldt, Error estimates for nonlinear finite element computations, *Computers Structures* **20**(1–3), 91–98 (1985).
26. O. C. Zienkiewicz, H. C. Huang and G. C. Liu, Adaptive FEM computation of forming process-application to porous and non-porous materials, *Int. J. Numer. Meth. Engng* **30,** 1527–1553 (1990).
27. H. H. Dannelongue and P. A. Tanguy, An adaptive remeshing technique for non-newtonian fluid flow, *Int. J. Numer. Meth. Engng* **30,** 1555–1567 (1990).
28. A. Chambarel and M. Pumborios, High-precision numerical simulation with autoadaptive grid technique in nonlinear thermal diffusion, *Numer. Heat Transfer B* **21,** 199–216 (1992).
29. H. C. Huang and R. W. Lewis, Adaptive analysis for heat flow problems using error estimation techniques, *Proceedings of the Sixth International Conference Numerical Methods in Thermal Problems*, Vol. 6, pp. 1029–1044. Pineridge Press, Swansea, U.K. (1989).
30. R. Lohner, An adaptive finite element scheme for transient problems in CFD, *Comput. Meth. Appl. Mech. Engng* **61,** 323–338 (1987).
31. R. Lohner, Adaptive remeshing for transient problems, *Comput. Meth. Appl. Mech. Engng* **75,** 195–214 (1989).
32. E. J. Probert, O. Hassan, K. Morgan and J. Peraire, Adaptive remeshing applied to the thermal analysis of a convectively cooled cylindrical leading edge, *Proceedings of the Seventh International Conference for Numerical Methods in Thermal Problems*, Vol. 7, pp. 811–823. Pineridge Press, Swansea, U.K. (1991).
33. R. W. Lewis, A. S. Usmani and J. T. Cross, Adaptive finite element analysis of heat transfer and flow problems, *Nonlinear Computational Mechanics—State of the Art*, Prof. Stein Memorial Volume, Springer, New York (1991).
34. R. A. Trompert, Local uniform grid refinement and systems of coupled partial differential equations, Report

NM-R9307, Centre for Mathematics and Computer Science, Amsterdam (1993).
35. A. S. Franca and K. Haghighi, Adaptive finite element analysis of transient thermal problems, *Numer. Heat Transfer B* **26**(3), 274–294 (1994).
36. E. Kang and K. Haghighi, A knowledge-based a priori approach to mesh generation in thermal problems, *Int. J. Numer. Meth. Engng* **35**, 915–937 (1992).
37. L. S. Oliveira, A. S. Franca and K. Haghighi, An adaptive approach to finite element modeling of drying problems, *Drying Technol.* (in press).
38. P. M. Gresho, R. L. Lee and R. L. Sani, On the time-dependent solution of the incompressible Navier-Stokes equations in two and three dimensions. In *Recent Advances in Numerical Methods in Fluids*, Vol. 1, pp. 27–79. Pineridge Press Limited, Swansea, U.K. (1980).
39. N. E. Bixler, An improved time integrator for finite element analysis, *Commun. Appl. Numer. Meth.* **5**, 69–78 (1989).
40. J. Irudayaraj, K. Haghighi and R. L. Stroshine, Nonlinear finite element analysis of coupled heat and mass transfer problems with an application to timber drying, *Drying Technol.* **8**(4), 731–749 (1990).